

# Effect of Carbon Particles on Aerodynamic Performance of a Radial Inflow Turbine in Closed Brayton Cycle

Ziyue MA, Pengfei LI, Shaojie ZHANG, Rong XIE\*, Jinguang YANG, Xiaofang WANG, Jinhu YANG

**Abstract:** For the closed Brayton cycle using carbon heaters, working fluid contains some solid particles generally. These impurities will enter turbine along with gas, influence aerodynamic performance, and even make turbine work under off-design condition. Therefore, it is necessary to study the influence of particles on turbine. In this paper, a turbine using argon with carbon particles as working fluid is investigated. Particles are assumed to have no volume and are evenly divided into ten different sizes. Based on the discrete phase model (DPM), CFD method is adopted to simulate turbine flow field, and influences of carbon particle mass fraction, particle diameter and incident velocity on aerodynamic performance are analyzed. The results indicate that as particle mass fraction increases, total pressure, static pressure and Mach number decrease significantly, isentropic efficiency decreases slightly, while temperature increases. Collision and rebound of particles in flow field are more intense with a larger particle diameter, but flow field is less influenced under the same mass fraction due to decrease of particle number. Incident velocity has little effect on aerodynamic performance; however, with increase of incident velocity, diameter of particles on blade surface is larger and collision of particles is more intense especially in nozzle. These results will help understand the influence of solid particles on turbines.

**Keywords:** discrete phase model; efficiency; particles; radial inflow turbine

## 1 INTRODUCTION

The massive consumption of fossil fuels not only brings about energy crisis, but also causes many environmental and climate problems. In addition to the development of alternative clean energy, one of the most practical and effective solutions is to improve the efficiency of energy utilization.

Closed Brayton cycles (CBC) with many benefits have potential to solve the above problems. Compared with conventional system, CBC can achieve higher efficiency with simpler equipment, and the choice of heat source as well as working fluids is more flexible [1]. CBC has been adopted in plenty of R&D programmes and commercially operated plants. In 1981, Research Center Juelich (KFA) in Germany built the high temperature helium turbomachine test facility (HHV) test system for the high temperature reactor helium gas turbine (HHT) project in collaboration of Germany, Switzerland, and the United States [2]. General Atomics (USA) and MINNATOM (Russia) made the plan in 1995 to develop and design the Gas Turbine-Modular Helium Reactor (GT-MHR) [3], which will be constructed in Russia at the Siberian Chemical Combine. The Gas Turbine High Temperature Reactor 300 (GTHTR300) program was proposed in 2001 for the purpose of developing a closed-cycle helium gas turbine [4]. In France, Framatone ANP, owned by AREVA and Siemens, developed the ANTARES (AREVA New Technology Advanced Reactor Energy Supply) hydrogen and electricity production concept [5]. Since the late 1990s, many institutes such as Sandia National Laboratories, Idaho National Laboratories, Argonne National Laboratories, Czech Technical University and Tokyo Institute of Technology, pay attention to the S-CO<sub>2</sub> cycle [6]. An 8MW CBC unit that converts waste heat into electricity using S-CO<sub>2</sub> working fluid was presented by Echogen in December 2014 as the first commercial application of S-CO<sub>2</sub> power cycles [1].

In a CBC as shown in Fig. 1 [7-10], working fluid is compressed to high pressure in compressor and is heated to high temperature in heater. Then, energy of fluid is

converted into power in turbine [11]. For the heat exchanger using carbon heaters, a small part of carbon is transformed into particles during heat transfer process and enters turbine along with the high-temperature and high-pressure fluid. Therefore, the fluid contains carbon particles when turbine is operating [12, 13]. With entrance of particles, service life, aerodynamic efficiency and cooling performance of blades decline seriously, which in turn affects safety [14], reliability and economy of the turbine. Moreover, with continuous increase of turbine inlet temperature and application of advanced cooling technology, the problem of particle flow in turbine becomes non-negligible and must be paid attention to.

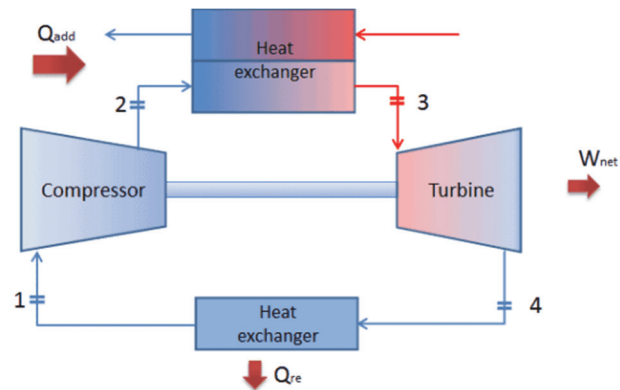


Figure 1 Process of closed Brayton cycle

Many researchers, such as Lv et al. [15], Aminjan et al. [16], and Feng et al. [17] have proposed integrated methods to analyze and design turbomachines. But these studies did not consider the presence of particles in the working fluid. Trajectory of solid particles in turbo-machinery is different from working fluid. Particles have different tracks and kinematic characteristics due to differences of particle diameter, mass, flow passage shape, and gas flow field property. Generally, effects of particles on turbine performance vary with mass fraction and particle diameter.

Han [18] adopted CFD method to calculate three-phase erosion flow. Compared with clean water condition, hydraulic efficiency of turbine under erosion condition

decreases, and the particles mixed in liquid-phase will disturb the water flow distribution on the working side of blade. Liu [19] used the DPM model to simulate erosion of particles on turbine blades, and found that capture efficiency of blades increases firstly and then decreases with particle size. Yao [20] employed the same method and suggested that as particle mass flow increases, the DPM erosion rate of blade increases significantly. Noon and Kim [21] explored the impact of different concentrations of sediment particles on the performance of Francis turbine and found that as the concentration increases, the efficiency loss of Francis turbine also increases. Ghenaiet [22] studied the trajectory of particles in a radial turbine and figured out that only small size particles travel easily through the rotor passage, whereas large particles only cross a small part of the rotor entry then are centrifuged back till reducing in size. Hu [23] took steam turbine as research object and explored motion status of different particle diameters in flow field. Trajectories of large particles are close to a straight line, and small particles mainly flow with the mainstream. In addition, Cao [24] and Roa [25] adopted steam turbines and water turbines as research objects respectively, and found that erosion rate is related to particle diameter and mass fraction of particles.

To sum up, mass fraction and diameter of particles have different effects on collision, erosion, and deposition in turbo-machinery. However, to the authors' knowledge, there are few researches on numerical simulations of the turbine with carbon particles in CBC. In order to provide a reference for engineering design, trajectory and collision of carbon particles in a radial turbine are simulated. Effects of carbon particle mass fraction, particle diameter and incident velocity on aerodynamic performance are analyzed.

## 2 NUMERICAL CALCULATION

### 2.1 Geometry Model and Meshing

The radial turbine investigated in this paper is derived from a test bed. Design parameters of the radial turbine after simplification are shown in Tab. 1.

**Table 1** Design parameters of the investigated turbine

Parameter	Value
Number of stator blades	19
Number of rotor blades	12
Inlet blade height/radius	5.6/40 / mm
Outlet (hub) blade height/radius	14/18 / mm
Outlet (shroud) blade height/radius	14/32 / mm
Ratio of tip clearance to blade height	1.43%

The geometry of the turbine is shown in Fig. 2. In order to reduce computation cost under the premise of accuracy, the periodic boundary technique is utilized to model a single-passage as shown in Fig. 3. Meshes on the blade surface, the tip gap and the wall surface are locally refined to ensure that boundary calculation data can be finely captured. The tip gap is set to 0.2 mm to capture tip leakage flow. Grid independence is verified by comparing the numerical simulation results under different grid numbers including 286101, 488672, 776672, 892480, and 1172416. Tab. 2 illustrates the dependence of aerodynamic performance on number of grids. It is observed that changes in each parameter become small when number of

grids is larger than 776672. Hence, the grid with number of grids being 776672 is taken for simulation.

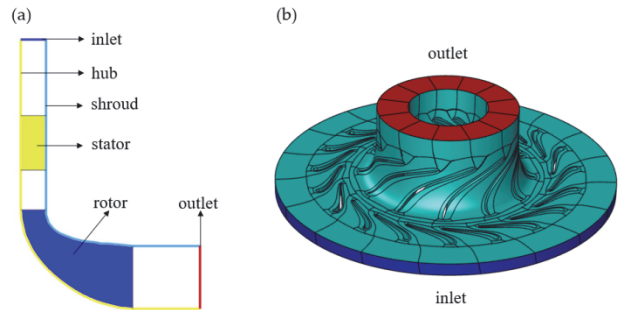


**Figure 2** (a) Meridian diagram; (b) 3D view of turbine

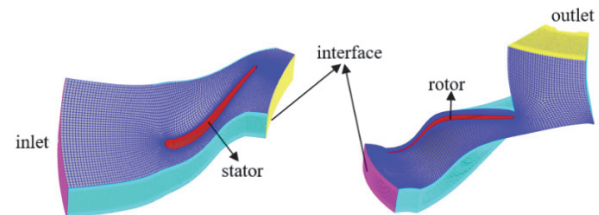


**Figure 3** Computational domain of the 3D radial turbine

**Table 2** Mesh independence analysis for the investigated turbine

Number of grids	Pressure ratio	Max y+	Mass flow rate / Kg/s	Mach number at outlet
286101	2.0438	87	0.838625	0.1648
488672	2.046	50	0.850777	0.1661
776672	2.0448	35	0.85398	0.1676
892480	2.044683	34	0.8522	0.1675
1172416	2.0443	34	0.85327	0.168

**Table 3** Turbine boundary condition setting

Type	Parameter setting
Inlet (Total temperature)	1140 / K
Inlet (Total pressure)	1740 / kPa
Outlet (Gauge pressure)	830 / kPa
Dynamic and static interface	Mixing plane
Period boundary	Rotation Period
Rotating speed	-90000 / rpm

In this paper, the standard  $k-\epsilon$  model is used as turbulence model and mixed gas of helium and xenon is the working fluid. Since physical parameters of this working fluid are similar to those of argon, furthermore, Liu's study [26] illustrated the flow similarity of argon and mixture of helium and xenon in a CBC. Argon can be used as working fluid in this study instead. The stator is set as a fixed fluid area and the rotor is set as a rotational fluid area with a speed of -90000 rpm. The mixing plane method is used to reflect genuine flow status. The boundary conditions of inlet and outlet are set as pressure inlet and pressure outlet. The boundary condition parameters are shown in Tab. 3.

### 2.2 Discrete Phase Model

The Discrete Phase Model (DPM) is based on the Euler-Lagrange approach [27-30]. The discrete phase is composed of spherical particles dispersed in the continuous phase. The fluid is managed as a continuous medium in simulation and described in the Eulerian coordinate system. The initial position, velocity, diameter and temperature of the particle are defined. Tracks of the discrete phase particles are solved by integrating the

differential equation of the particle force in the Lagrangian coordinate system, and trajectory of particles and the heat and mass transfer caused by particles can be calculated (Somwangthanaroj and Fukuda, 2020). Assuming that particles have no volume in fluid motion, collisions between particles can be ignored [30, 31]. Therefore, the DPM is applicable as long as the fluid is with a low volume fraction of discrete phase.

Core of the DPM model is using the Newton's second law to calculate tracks of particles in fluid. In the Lagrangian coordinate system, tracks of discrete phase particles (droplets or bubbles) are predicted by integrating the dynamic equilibrium equation of particles. This dynamic equilibrium equates the inertia of particle with the force acting on particle, which can be written as:

$$m_p \frac{d\vec{u}_p}{dt} = \sum_i \vec{F}_i \quad (1)$$

where  $m_p$ ,  $\vec{u}_p$ ,  $\vec{F}$  denote mass of particles, the velocity of discrete phase, different types of forces exerted on particles in flow. Generally speaking, the force acting on particles consists of drag force, gravity, Brownian Force, Saffman Lift Force, Magnus Force and Thermophoretic Force, etc.

Rotation of particles is also a type of motion in flow field, which has a great influence on the trajectory of particles. For large particles or heavy particles with a high moment of inertia, the effect is more pronounced. Therefore, rotation of particles cannot be ignored in simulation. Considering the rotation of particles, additional ordinary differential equation of particle angular momentum is solved by:

$$I_p \frac{d\omega_p}{dt} = \frac{\rho_f}{2} \left( \frac{d_p}{2} \right)^5 C_\omega |\vec{\Omega}| \cdot \vec{\Omega} = \vec{T} \quad (2)$$

where  $I_p$ ,  $\omega_p$ ,  $\rho_f$ ,  $d_p$ ,  $C_\omega$ ,  $\vec{T}$  denote moment of inertia, particle angular velocity, fluid density, particle diameter, rotation drag coefficient and torque applied to the particles in the fluid domain, respectively.  $\vec{\Omega}$  denotes relative particle-fluid angular velocity which is computed by:

$$\vec{\Omega} = \frac{1}{2} \nabla \times \vec{u}_f - \vec{\omega}_p \quad (3)$$

For spherical particles, the formula for calculating the moment of inertia is:

$$I_p = \frac{\pi}{60} \rho_p d_p^5 \quad (4)$$

It is obvious that torque  $\vec{T}$  is produced by the balance between particle inertia and resistance.

Heat transfer between particles and fluid follows the heat transfer equation:

$$m_p C_p \frac{dT_p}{dt} = h_c A_p (T_f - T_p) \quad (5)$$

where  $A_p$ ,  $C_p$ ,  $T_p$ ,  $T_f$ ,  $h_c$  denote particle surface area, isobaric specific heat capacity, particles temperature, fluid temperature and convective heat transfer coefficient between particles and fluid, respectively. Because particles stay on the wall for a relatively short time and the temperature of particles is not much different from the temperature of gas, heat transfer between particles and wall is not calculated.

In this paper, carbon particles are taken as the research object. The discrete phase is coupled with flow field, and the steady-state tracking method is adopted. The particles are injected from the inlet by surface injection. When calculating the particle track, it is necessary to consider collision between particles and wall (Ghenaït et al., 2010). Because kinetic energy of particles is partially lost after rebound, size and direction of particle velocity will change. The movement type at inlet and outlet is set to escape, and the movement type of the particles on the wall is set to reflection. Since carbon particles are mixed into fluid and the volume fraction of particles is small, the particle temperature and flow rate can be set to be same as the fluid. Particle size entering the turbine is generally concentrated in tens of microns (Liu et al., 2021; Hamed et al., 2006). In order to analyze the influence of particles on aerodynamic performance of turbine directly, the simulation with 0.5%, 5% and 10% mass fraction of carbon particles are carried out respectively. Mass fraction of the particles can be determined according to the mass flow rate of radial turbine under different working conditions.

### 3 RESULTS AND DISCUSSION

#### 3.1 Validation of Numerical Method

To validate accuracy of the CFD method adopted in this study, the CFD results are compared against the experimental data of a Brayton-cycle turbine using argon as working fluid. Details of the turbine geometry and test conditions are listed in Reference [32].

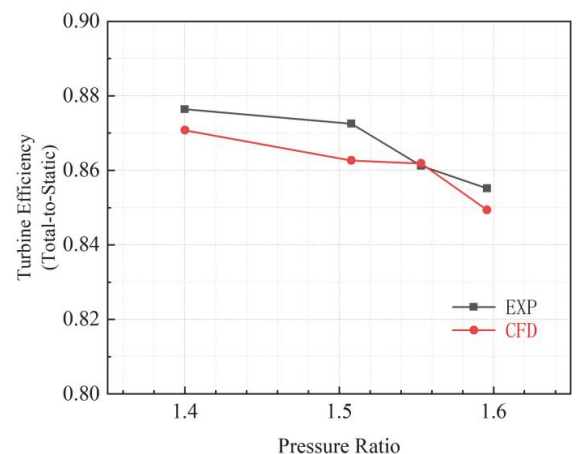


Figure 4 Comparison between CFD results and experimental data

Comparison of calculated efficiency and test values under different pressure ratios are shown as Fig. 4. The maximum of deviation between CFD results and experimental data is less than 1%. It indicates good consistence between prediction and experiment.

### 3.2 Influence of Particle Mass Fraction on Turbine Performance

Mass fraction of carbon particles which are generated in carbon heater and flow into radial turbine may change over time. In order to explore the effect of particle mass fraction on turbine performance, three flow fields with different mass fractions of particles are selected for comparison. First, steady three-dimensional numerical simulation for a radial turbine is performed to obtain the aerodynamic parameters of flow field. After argon flows through the stator, variation of total pressure and total temperature is little, while static pressure and Mach number change greatly, and speed rises in stator passage rapidly. There is almost no change in aerodynamic parameters at the interface of stator and rotor. Total pressure, static pressure, temperature and Mach number in the rotor flow passage change dramatically, and flow rate decreases gradually as the fluid flows. Carbon particles with mass fractions of 0.5%, 5%, and 10% are added to fluid respectively and these conditions are compared with the initial flow field. It can be seen from Fig. 5 and Fig. 6 that as particle mass fraction increases, temperature in flow field increases, and this effect is extremely obvious at the outlet.

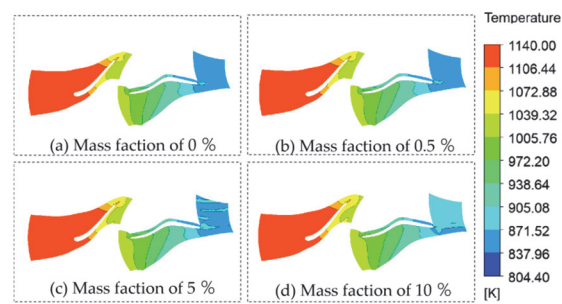


Figure 5 Temperature distribution at 50% blade height with different mass fraction of particles

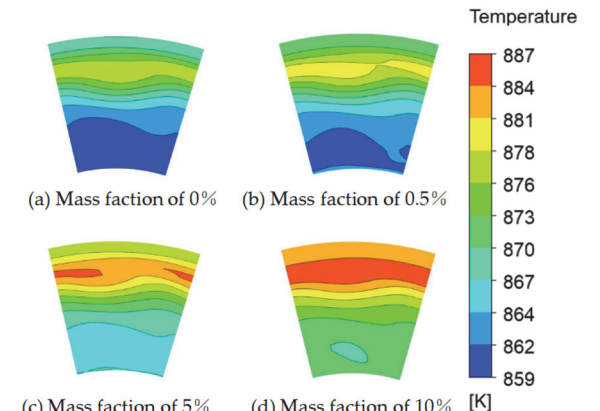


Figure 6 Outlet temperature distribution with different mass fraction of particles

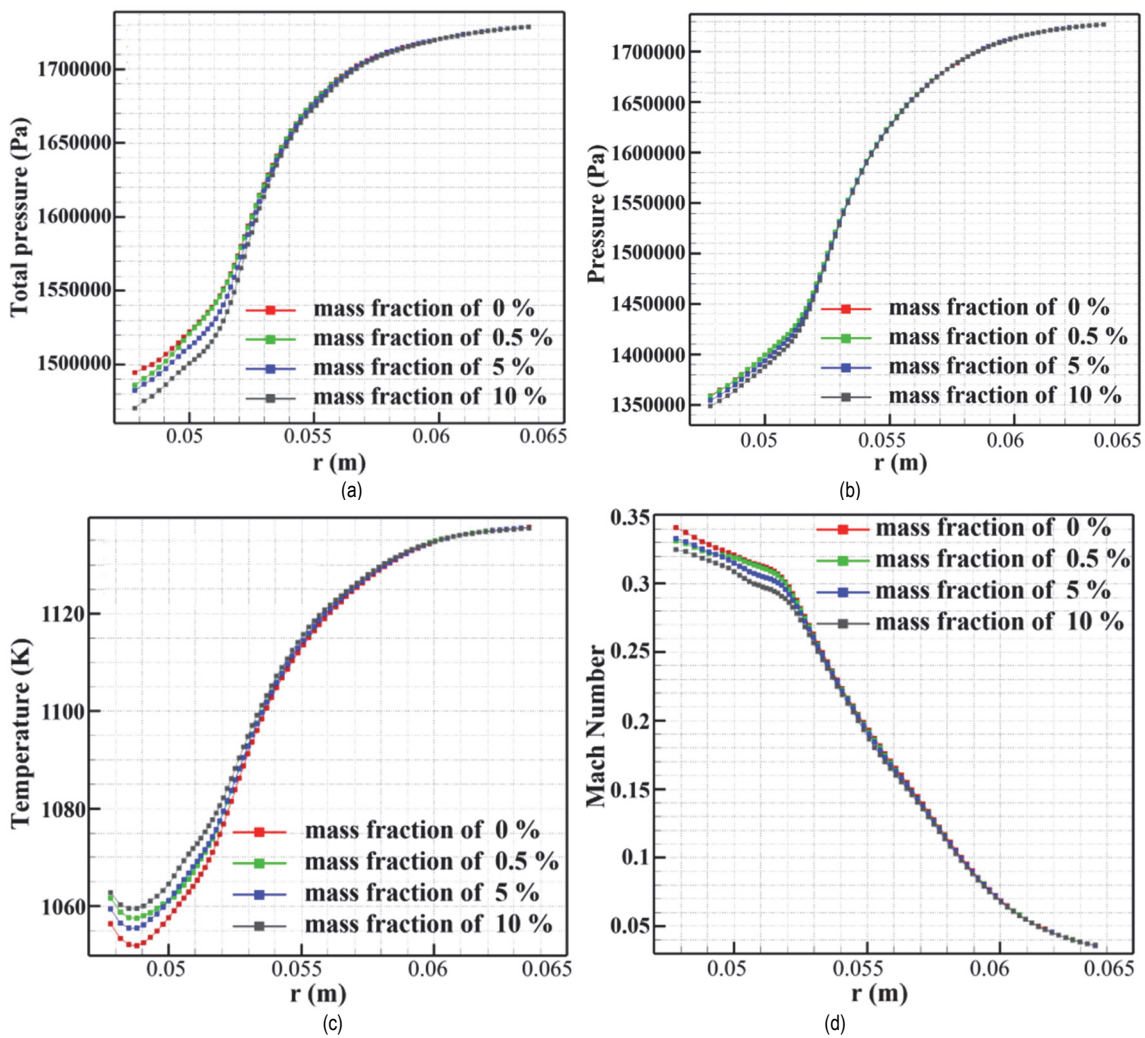
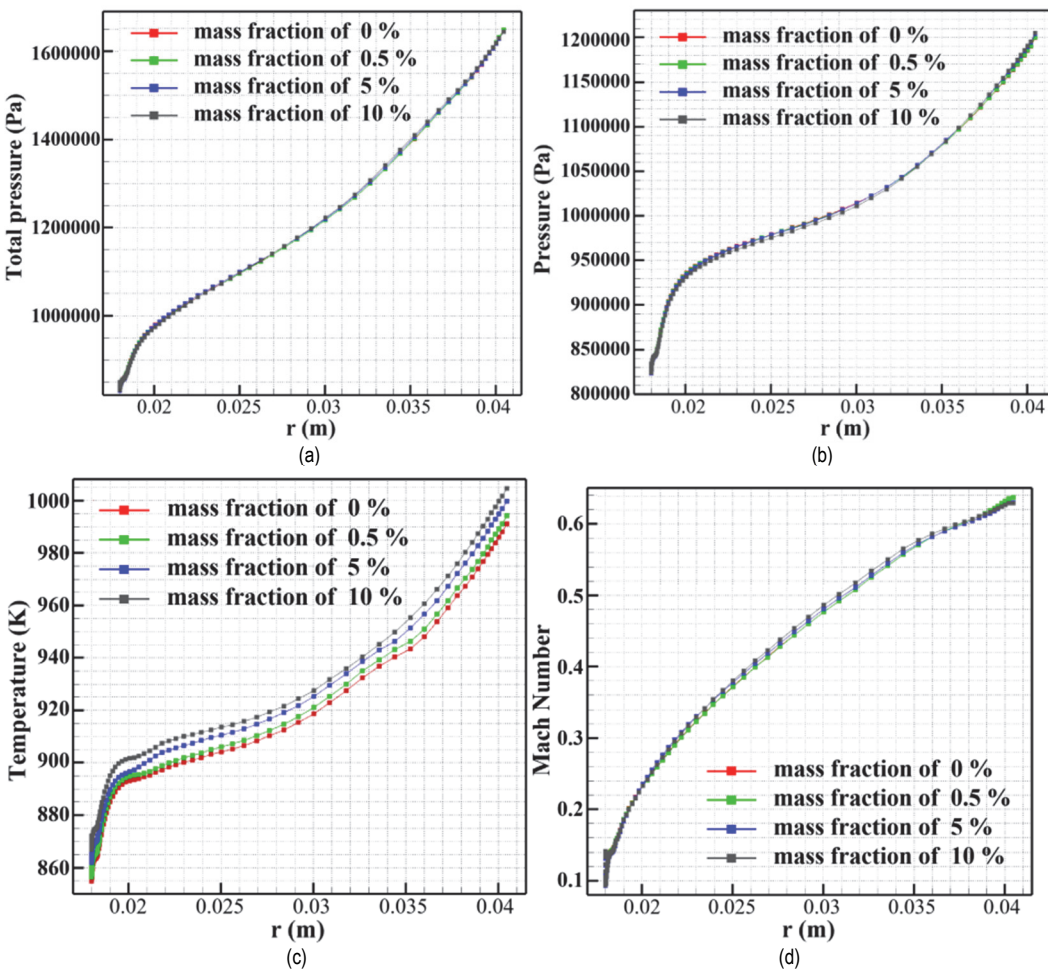
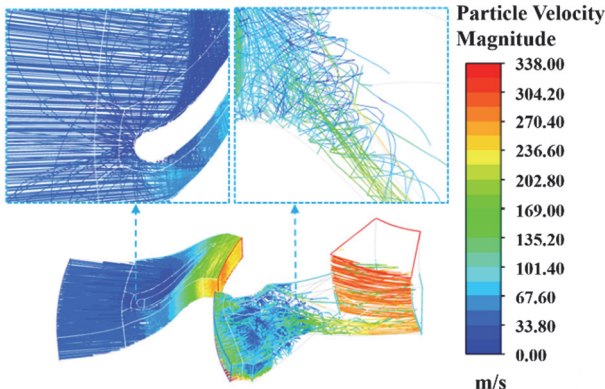


Figure 7 Comparison of thermodynamic parameters with different mass fraction of particles in stator: (a) total pressure; (b) static pressure; (c) temperature; (d) Mach number



**Figure 8** Comparison of thermodynamic parameters with different mass fraction of particles in rotor: (a) total pressure; (b) static pressure; (c) temperature; (d) Mach number

Streamlines are selected near the stator and rotor blades. Along these streamlines, comparisons of total pressure, static pressure, temperature and Mach number are shown in Fig. 7 and Fig. 8.



**Figure 9** Carbon particle velocity distribution

It can be seen from the above results that aerodynamic parameters change with mass fraction of particles. In order to analyse relationship between aerodynamic parameters and particles quantitatively, dimensionless aerodynamic parameters at interface are shown in Fig. 10.

At interface, with increase of mass fraction of carbon particles, total pressure, static pressure and Mach number decreased obviously while temperature increased, and the effect is more significant as mass fraction gets greater.

Aerodynamic parameters at the interface change in the same way with that in stator and rotor passage. Collision and rebound of particles in flow passage will cause energy loss and reduction of velocity. This part of energy is converted into heat and absorbed by fluid, thus temperature of the fluid gradually rises with the increase of mass fraction of particles.

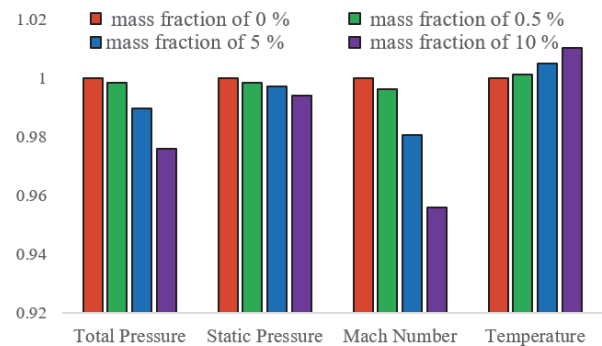


**Figure 10** Dimensionless aerodynamic parameters of different mass fractions of particle at interface

Isentropic efficiency is a key parameter to evaluate a turbine performance. Carbon particles are added to flow field of a radial turbine under different operating conditions to investigate the effect of mass fraction of carbon particles on turbine efficiency. Five operating conditions with pressure drop ratio of 1.8, 2.1, 2.5, 3.0 and 4.0 are calculated. Compared with data of initial flow field,

the performance curves shown in Fig. 11 and Fig. 12 can be obtained:

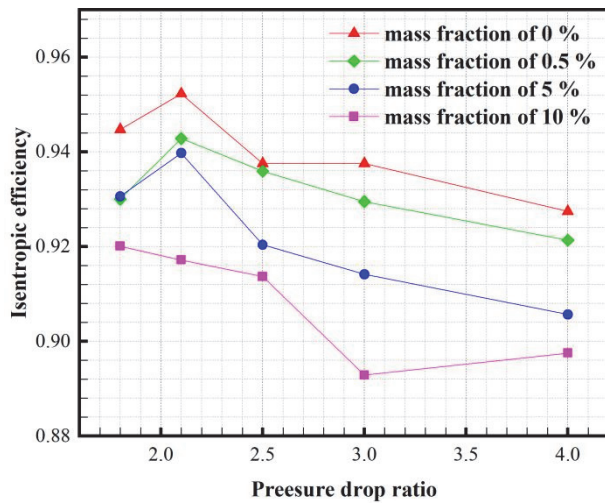


Figure 11 Variation of isentropic efficiency with pressure ratio under different mass fractions of particle

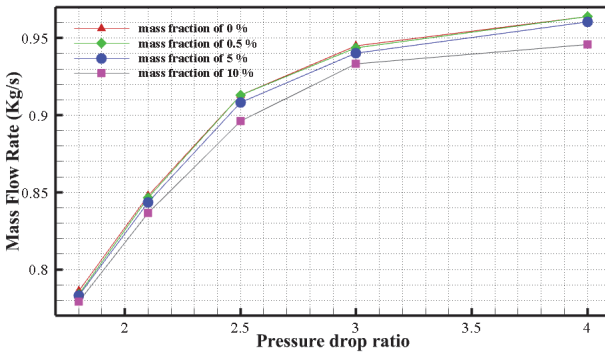


Figure 12 Variation of mass flow rate with pressure ratio under different mass fractions of particle

1. After adding carbon particles with different mass fractions, the isentropic efficiency of turbine under each working condition has a significant drop. The greater the mass fraction, the more the isentropic efficiency decreases, and the decrease is greatest when the pressure ratio is 3.0. The reason for this phenomenon is caused by changes in parameters such as total pressure and total temperature of the flow field.

2. After adding carbon particles, the mass flow rate decreases with the increase of carbon particle mass fraction. Mass flow rate does not change significantly as mass fraction of carbon particles is 0.5%. When mass fraction is 5% and 10%, the mass flow rate decreases significantly and is most affected at a pressure drop ratio of 4.0. The increased flow resistance is a result of a higher apparent viscosity of the fluid due to the increased mass fraction of particles.

### 3.3 Influence of Particle Diameter on Performance of Radial Turbine

In order to investigate the effect of particle diameter on turbine performance, average diameter of particles was taken as 0.01 mm, 0.03 mm, 0.05 mm, 0.07 mm and 0.09 mm respectively.

Particle Stokes number is a function of particle diameter and density, it is defined as  $St = \tau_p/\tau_f$  in Eqs. (6) and (7) and is used to describe the ability particle entrainment carried by the gas phase (Fra et al., 2020).

$$\tau_p = \frac{1}{18} \frac{\rho_p d_p^2}{\mu_g} \quad (6)$$

$$\tau_f = \frac{L_{\text{char}}}{U_{\text{char}}} \quad (7)$$

where  $\rho_p$ ,  $d_p$ ,  $\mu_g$ ,  $L_{\text{char}}$ ,  $U_{\text{char}}$  denote density, diameter of discrete phase, viscosity of fluid, Characteristic length and Characteristic velocity of particles.

When particle diameter is small, Stokes number is also small, and most of the particles can flow with fluid, so rebound of particle is weak, and the particle trajectory is relatively regular. As particle diameter increases, Stokes number becomes larger, the ability of particles to flow with the fluid becomes worse, rebound and collision of particles become stronger, and particle trajectory becomes irregular. This phenomenon can be clearly observed from the red dashed box in Fig. 13.

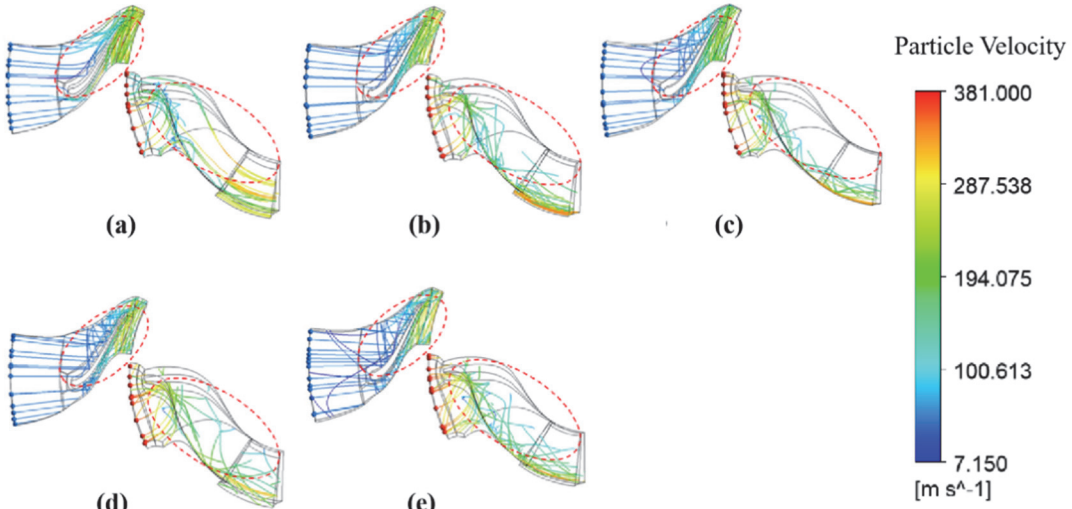


Figure 13 Trajectory of particles with different diameters at mass fraction of 5%: (a)  $d = 0.01 \text{ mm}$ , (b)  $d = 0.03 \text{ mm}$ , (c)  $d = 0.05 \text{ mm}$ , (d)  $d = 0.07 \text{ mm}$ , (e)  $d = 0.09 \text{ mm}$

Fig. 14 shows the variation of isentropic efficiency and mass flow rate with average diameter of particles. It indicates that isentropic efficiency and mass flow rate increase with particle diameter. Main reason is that when mass fraction of carbon particles is constant, number of particles increases with the decrease of particle diameter and more particles are distributed in flow field, which will enhance the influence of particles. Conversely, the larger the particle diameter, the smaller the number of particles, and the weaker the influence on flow field.

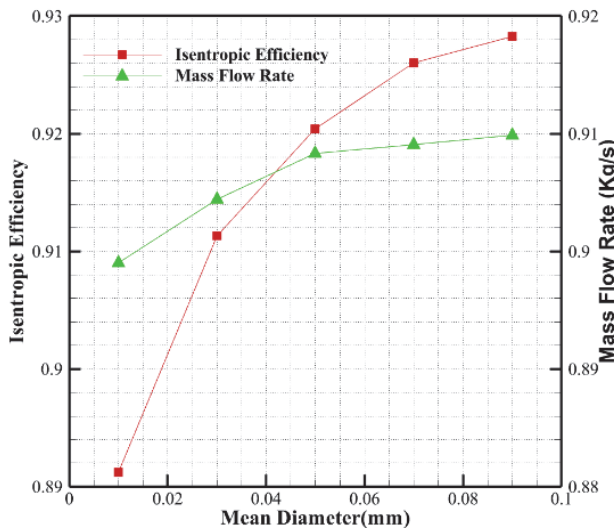


Figure 14 Variation of Performance with average particle diameter at a pressure ratio of 2.5

### 3.4 The Effect of Particle Incident Velocity on Particle Motion

As carbon particles flow into turbine with fluid, particles' rate cannot be determined. If the pipeline between carbon heater and turbine is long enough, the particles will enter turbine at the same velocity as the fluid. When particles cannot be accelerated sufficiently to the same velocity as fluid, it may not be able to truly express the motion of particles. In this paper, half of fluid velocity is taken as the particle velocity. The results show that incident velocity of particles has little effect on performance of turbine and aerodynamic parameters of flow field. Variation of isentropic efficiency and mass flow rate with pressure ratio at two incident velocities is shown in Fig. 15.

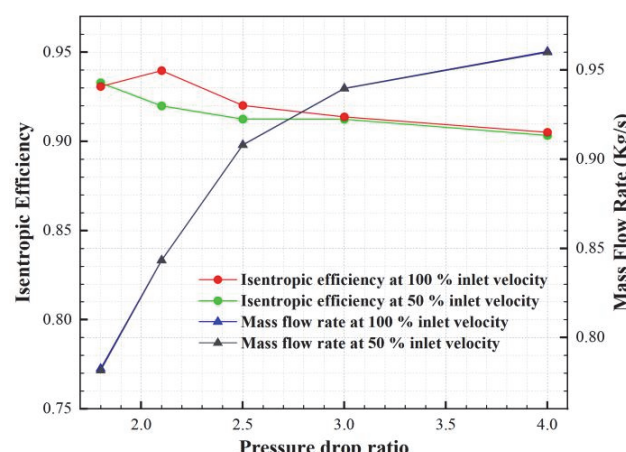


Figure 15 Mass flow rate and isentropic efficiency curves at different velocities

It can be seen that there is little difference in isentropic efficiency between two velocities while the difference of mass flow rate is negligible.

The incident velocity of particles will affect particle trajectory, particle collision and particle diameter distribution. It can be seen from Fig. 16 that at a small incident velocity of particles, particles reflect after hitting the wall with small reflection angle and trajectories of particles are relatively regular. When incident velocity of particles becomes larger, the reflection angle increases and the trajectories become denser and irregular. This phenomenon is more obvious in stator flow passage, because particle velocity will gradually increase to the velocity of main flow, and fluid velocity in the rotor is almost the same as the particle velocity. In addition, incident velocity can also affect particle diameter distribution on blade surface. It can be seen from Fig. 17 that particle diameter on blade surface is larger with a larger particle velocity. This phenomenon is particularly obvious at the leading edge of the suction surface of stator blade. This is due to the increase of collision which makes many large particles deposit on the surface of blade.

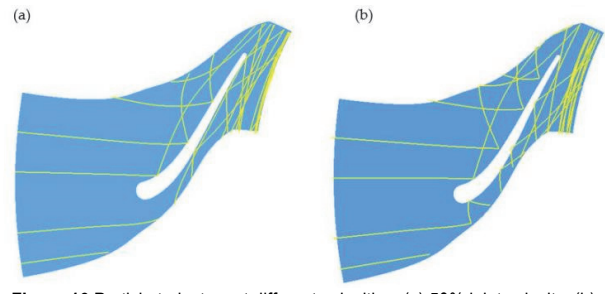


Figure 16 Particle trajectory at different velocities: (a) 50% inlet velocity; (b) 100% inlet velocity

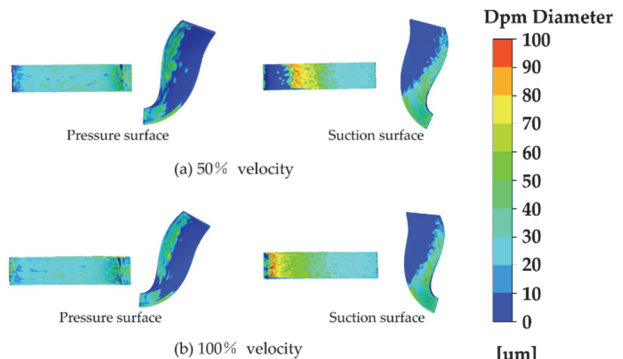


Figure 17 The particle diameter distribution on the blade surface at different velocities: (a) 50% inlet velocity; (b) 100% inlet velocity

## 4 CONCLUSIONS

To fill the gap of study of the influence of carbon particles in a radial turbine, based on the DPM model, CFD method is adopted in this paper to study the effects of carbon particles. Compared to the existing studies, influences of mass fraction, particle diameter and incident velocity on the flow field and performance of a radial turbine are investigated. The main conclusions are as follows:

(1) Influence of carbon particles on flow field of a radial turbine is studied by adding carbon particles of different mass fraction into the turbine and comparing flow

field with initial condition. With the entrance of particles, total pressure, static pressure and Mach number decrease and temperature increases. Centrifugal force in rotor will weaken this influence. The existence of particulate impurities in turbine will disturb flow field, even make turbine to work under off-design conditions as the particle fraction is large enough.

(2) Isentropic efficiency and mass flow rate of turbine decrease with particle mass fraction and the effect is more significant as mass fraction gets greater.

(3) When particle mass fraction is constant, impact of particles on flow field lessens with the increase of particle diameter. A larger particle diameter makes particles more difficult to drift with main fluid. Therefore, rebound and collision of particles in flow field are intense and trajectories of particles are more irregular.

(4) The incident velocity of particles has almost no effect on the aerodynamic parameters of a radial turbine flow field, but collisions and reflection angle of particles increase with the velocity, and particle diameter on blade surface is larger.

## Acknowledgements

Supported by the Taishan Scholars Program.

## 5 REFERENCES

- [1] Olumayegun, O., Wang, M., & Kelsall, G. (2016). Closed-cycle gas turbine for power generation: A state-of-the-art review. *Fuel*, 180, 694-717. <https://doi.org/10.1016/j.fuel.2016.04.074>
- [2] Weisbrodt, I. A. (1996). *Summary report on technical experiences from high-temperature helium turbomachinery testing in Germany*.
- [3] Kiryushin, A. I., Kodochigov, N. G., Kouzavkov, N. G., Ponomarev-Stepnoi, N. N., Gloushkov, E. S., & Grebennik, V. N. (1997). Project of the GT-MHR high-temperature helium reactor with gas turbine. *Nuclear Engineering and design*, 173(1-3), 119-129. [https://doi.org/10.1016/S0029-5493\(97\)00099-X](https://doi.org/10.1016/S0029-5493(97)00099-X)
- [4] Yan, X., Kunitomi, K., Nakata, T., & Shiozawa, S. (2003). GTHTR300 design and development. *Nuclear Engineering and Design*, 222(2-3), 247-262. [https://doi.org/10.1016/S0029-5493\(03\)00030-X](https://doi.org/10.1016/S0029-5493(03)00030-X)
- [5] Carre, F., Yvon, P., Anzieu, P., Chauvin, N., & Malo, J. Y. (2010). Update of the French R&D strategy on gas-cooled reactors. *Nuclear Engineering and Design*, 240(10), 2401-2408. <https://doi.org/10.1016/j.nucengdes.2010.02.042>
- [6] Dostal, V., Todreas, N. E., Hejzlar, P., & Kazimi, M. S. (2002). *Power conversion cycle selection for the LBE cooled reactor with forced circulation*. MIT-ANP-TR-085.
- [7] Yuan, Z., Zheng, Q., Yue, G., & Jiang, Y. (2021). Performance evaluation on radial turbines with potential working fluids for space closed Brayton cycle. *Energy Conversion and Management*, 243, 114368. <https://doi.org/10.1016/j.enconman.2021.114368>
- [8] Hosseinpour, J., Howard, J., Chen, J., & Engeda, A. (2021). Challenges for Developing and Marketing a Brayton-Cycle-Based Power Genset Gas Turbine Using Supercritical CO<sub>2</sub> and a Compressor Design for Simple Recuperated Cycle. *Journal of Energy Resources Technology*, 144, 032101. <https://doi.org/10.1115/1.4051305>
- [9] Uusitalo, A., Turunen-Saaresti, T., & Grönman, A. (2021). Design and loss analysis of radial turbines for supercritical CO<sub>2</sub> Brayton cycles. (2021). *Energy*, 230, 120878. <https://doi.org/10.1016/j.energy.2021.120878>
- [10] Wang, X., Wang, R., Bian, X., Cai, J., Tian, H., Shu, G., Li, X., & Qin, Z. (2021). Review of dynamic performance and control strategy of supercritical CO<sub>2</sub> Brayton cycle. *Energy and AI*, 100078. <https://doi.org/10.1016/j.egyai.2021.100078>
- [11] Gharehdaghi, S., Moujaes, S. F., & Nejad, A. M. (2021). Thermal-fluid analysis of a parabolic trough solar collector of a direct supercritical carbon dioxide Brayton cycle: A numerical study. *Solar Energy*, 220, 766-787. <https://doi.org/10.1016/j.solener.2021.03.039>
- [12] Panakarajupally, R. P., Mirza, F., Rassi, J. E., Morscher, G. N., Abdi, F., & Choi, S. (2021). Solid particle erosion behavior of melt-infiltrated SiC/SiC ceramic matrix composites (CMCs) in a simulated turbine engine environment. *Composites Part B: Engineering*, 216, 108860. <https://doi.org/10.1016/j.compositesb.2021.108860>
- [13] Hamed, A. (1992). An investigation in the variance in particle surface interactions and their effects in gas turbines. *Journal of Engineering for Gas Turbines and Power*, 114, 235-241. <https://doi.org/10.1115/1.2906578>
- [14] Lawson, S. A., Thole, K. A., Okita, Y., & Nakamata, C. (2012). Simulations of multiphase particle deposition on a showerhead with staggered film-cooling holes. *Journal of Turbomachinery*, 134, 051041. <https://doi.org/10.1115/1.4004757>
- [15] Lv, G., Yang, J., Shao, W., & Wang, X. (2018). Aerodynamic design optimization of radial-inflow turbine in supercritical CO<sub>2</sub> cycles using a one-dimensional model. *Energy conversion and management*, 165, 827-839. <https://doi.org/10.1016/j.enconman.2018.03.005>
- [16] Aminjan, K. K., Heidari, M., Rahmaniavahid, P., Alipour, H., & Khashehchi, M. (2021). Design and simulation of radial flow turbine impeller and investigation thermodynamic properties of flow in LE and TE. *TEM Journal*, 10(2), 975. <https://doi.org/10.18421/TEM102-62>
- [17] Feng, Z., Deng, Q., & Li, J. (2005, January). Aerothermodynamic design and numerical simulation of radial inflow turbine impeller for a 100kW microturbine. *Turbo Expo: Power for Land, Sea, and Air*, 46997, 873-880. <https://doi.org/10.1115/GT2005-68276>
- [18] Han, L., Wang, Y., Zhang, G. F., & Wei, X. Z. The particle induced energy loss mechanism of Pelton turbine. (2021). *Renewable Energy*, 173, 237-248. <https://doi.org/10.1016/j.renene.2021.03.136>
- [19] Liu, Z., Diao, W., Liu, Z., & Zhang, F. (2021). A Numerical Study of the Effect of Particle Size on Particle Deposition on Turbine Vanes and Blades. *Advances in Mechanical Engineering*, 13(5), 021033-234. <https://doi.org/10.1177/16878140211017812>
- [20] Yao, Y., Bai, X., Liu, H., Li, T., Liu, J., & Zhou, G. (2021). Solid Particle Erosion Area of Rotor Blades: Application on Small-Size Unmanned Helicopters. *Symmetry*, 13(2), 178. <https://doi.org/10.3390/sym13020178>
- [21] Noon, A. A. & Kim, M. H. (2017). Erosion wear on Francis turbine components due to sediment flow. *Wear*, 378-379, 126-135. <https://doi.org/10.1016/j.wear.2017.02.040>
- [22] Ghenaiet, A. (2010). Prediction of Erosion in Radial Turbine Components. *Turbo Expo: Power for Land, Sea, and Air*, 44021, 1831-1846. <https://doi.org/10.1115/GT2010-22419>
- [23] Hu, P. F., Li, Y., Cao, L. H., & Zhang, T. (2017). Analysis on Solid Particle Erosion in the Governing Stage of a High-Parameter Steam Turbine. *Turbo Expo: Power for Land, Sea, and Air*, 50954, V008T29A022. <https://doi.org/10.1115/GT2017-63946>
- [24] Cao, L., Liu, S., Hu, P., & Si, H. (2020). The influence of governing valve opening on the erosion characteristics of solid particle in steam turbine. *Engineering Failure Analysis*, 118, 104929. <https://doi.org/10.1016/j.engfailanal.2020.104929>

- [25] Roa, C. V., Muñoz, J., Teran, L. A., Valdes, J. A., Rodríguez, S. A., Coronado, J. J., & Ladino, A. (2015). Effect of tribometer configuration on the analysis of hydro machinery wear failure. *Wear*, 332, 1164-1175.  
<https://doi.org/10.1016/j.wear.2015.01.068>
- [26] Liu, X. (2019). *Investigation on Aerodynamic Design and Flow Characteristics of Centrifugal Compressor Using Helium and Xenon*. Master's thesis, Harbin Engineering University.
- [27] Zahari, N. M., Zawawi, M. H., Sidek, L. M., Mohamad, D., Itam, Z., Ramli, M. Z., Syamsir, A., Abas, A., & Rashid, M. (2018). Introduction of discrete phase model (DPM) in fluid flow: A review. *AIP Conference Proceedings*, 2030, 020234.  
<https://doi.org/10.1063/1.5066875>
- [28] Somwangthanaroj, S. & Fukuda, S. (2020). CFD modeling of biomass grate combustion using a steady-state discrete particle model (DPM) approach. *Renewable Energy*, 148, 363-373. <https://doi.org/10.1016/j.renene.2019.10.042>
- [29] Hwang, I. S., Jeong, H. J., & Hwang, J. (2019). Numerical simulation of a dense flow cyclone using the kinetic theory of granular flow in a dense discrete phase model. *Powder Technology*, 356, 129-138.  
<https://doi.org/10.1016/j.powtec.2019.08.008>
- [30] Zhu, L., Li, A., & Wang, Z. (2018). Analysis of particle trajectories in a quick-contact cyclone reactor using a discrete phase model. *Separation Science and Technology*, 53, 928-939.  
<https://doi.org/10.1080/01496395.2017.1386683>
- [31] Mingzhi, Z., Yiming, M., & Xiaobo, K. (2018). Base on DPM model to simulation Sand erosion on PV modules surface. *IOP Conference Series: Earth and Environmental Science*, 012036.  
<https://doi.org/10.1088/1755-1315/146/1/012036>
- [32] Jack, A. H. (1965). *Design and fabrication of a Brayton-cycle turbine research package*. NASA.

#### Contact information:

**Ziyue MA**, Doctor  
 School of Energy and Power, Dalian University of Technology,  
 Dalian 116024, China  
 E-mail: baziyue21@gmail.com

**Pengfei LI**, Assistant Master  
 School of Energy and Power, Dalian University of Technology,  
 Dalian 116024, China  
 E-mail: pengfeili@mail.dlut.edu.cn

**Shaojie ZHANG**, Master  
 School of Energy and Power, Dalian University of Technology,  
 Dalian 116024, China  
 E-mail: 745102371@qq.com

**Rong XIE**, Associate Professor  
 (Corresponding author)  
 School of Energy and Power, Dalian University of Technology,  
 Dalian 116024, China  
 E-mail: xieronz@dlut.edu.cn

**Jinguang YANG**, Professor  
 School of Energy and Power, Dalian University of Technology,  
 Dalian 116024, China  
 E-mail: jinguang\_yang@dlut.edu.cn

**Xiaofang WANG**, Professor  
 School of Energy and Power, Dalian University of Technology,  
 Dalian 116024, China  
 E-mail: dlwxf@dlut.edu.cn

**Jinhu YANG**, Professor  
 Qingdao Institute of Aeronautical Technology,  
 Qingdao 266404, China  
 E-mail: yangjinhu@iet.cn